Electronic Supplementary Information (ESI)

Evaluating the component contribution to the nonlinear optical performances using stable [Ni_4O_4] cuboidal clusters as models

Zhi-Min Hao,[a] Meng-Yao Chao,[a] Yan-Liu,[a] Ying-Lin Song,[b] Jun-Yi Yang,*[b] Lifeng Ding,*[c] Wen-Hua Zhang*[a] and Jian-Ping Lang*[a]

[a] *College of Chemistry, Chemical Engineering and Materials Science, Soochow University, Suzhou 215123, China; E-mail: whzhang@suda.edu.cn; jplang@suda.edu.cn*

[b] *College of Physics, Optoelectronics, and Energy, Soochow University, Suzhou 215006, China; E-mail: yjy2010@suda.edu.cn*

[c] *Department of Chemistry, Xi'an Jiaotong-Liverpool University, Suzhou 215123, China; E-mail: lifeng.ding@xjtlu.edu.cn*

Table of Contents

1. Syntheses of 1–5

Materials and methods

Nickel chloride ($NiCl_2$, 98%), nickel bromide hexahydrate ($NiBr_2{\cdot}6H_2O$, 96%), 2-(hydroxymethyl)-4-aminopyridine (L_{NH_2}, 99%), 4-chloro-2-pyridinemethanol (L_{Cl}, 99%), 5-bromo-2-pyridinemethanol (L_{Br}, 99%) and other chemicals used in this work were commercially available and without further purifications. IR spectra were measured on a Varian 1000 FT-IR spectrometer as KBr disks (400 – 4000 cm^{-1}). Elemental analyses for C, H and N were carried out on a Carlo-Erba CHNO-S microanalyzer. Thermogravimetric analyses were performed with a Mettler Toledo Star system (heating rate of 5 °C min^{-1}). The UV-Vis absorption spectra were obtained on a Varian Cary-50 UV-visible spectrophotometer. Electrospray ionization mass spectrometries (ESI-MS) were performed on an Agilent 1200/6200 mass spectrometer using MeOH as the mobile phase. The NLO analysis was measured by using the Z-scan test technology under the conditions of wavelength for 532 nm, pulse width of 15 ps.

Synthetic schemes

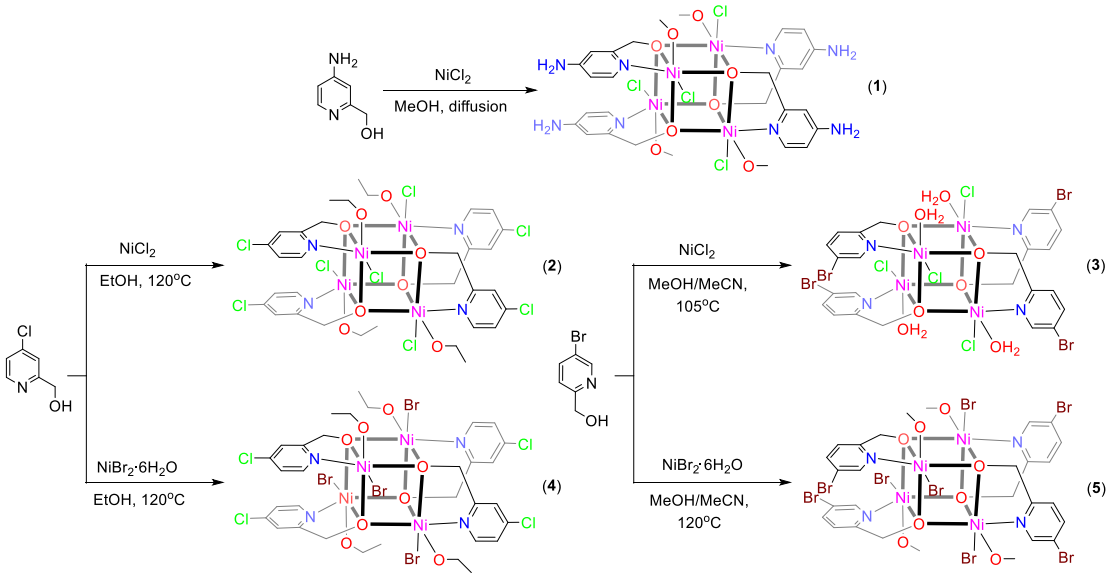

Scheme S1 Synthetic routes for clusters **1**–**5**.

Synthesis of $[Ni_4(L_{NH_2})_4Cl_4(MeOH)_4]$ (**1**)

Adding 2-(hydroxymethyl)-4-aminopyridine (L_{NH_2}, 24 mg, 0.2 mmol) and $NiCl_2$ (26 mg, 0.2 mmol) in MeOH (20 mL) resulted in a light blue solution which was stirred for 4 hours. The resulting mixture was centrifuged and the supernatant fluid diffused with Et_2O to give blue block crystals of **1** after a week. Yield: 13 mg (26.1% based on Ni). Anal. Calcd. (%) for $C_{28}H_{44}Cl_4N_8Ni_4O_8$: C 28.11, H 4.42, N 10.80; found: C 28.67, H 4.79, N 10.69. IR (KBr disc): 3280 (m), 2844 (w), 1631 (s), 1560 (w), 1497 (m), 1465 (w), 1272 (m), 1065 (s), 1023 (s), 940 (w), 831 (w), 683 (w) cm^{-1}. UV-Vis (DMSO, λ_{max} (nm (ε $M^{-1}cm^{-1}$))): 403.94 (14438), 532 (663), 658.95(5661.6).

Synthesis of $[Ni_4(L_{Cl})_4Cl_4(EtOH)_4]$ (**2**)

A mixture of $NiCl_2$ (26 mg, 0.2 mmol), 4-chloro-2-pyridinemethanol (L_{Cl}, 29 mg, 0.2 mmol) and EtOH (10 mL) was sealed in a Pyrex glass tube and smoothly heated to 120 °C within 4 h and maintained for 72 h before cooling to room temperature in 48 h to give green block single crystals, which were collected by filtration, washed thoroughly with EtOH, and dried in vacuo. Yield: 23.4 mg (41.4% based on Ni). Anal. Calcd. (%) for $C_{32}H_{44}Cl_8N_4Ni_4O_8$: C 27.97, H 2.92, N 5.70; found: C 27.99, H 3.17, N 5.59. IR (KBr disc): 3363 (m), 2899 (w), 2841 (w), 1594 (s), 1555 (m), 1472 (m), 1403 (w), 1205 (m), 1078 (s), 1020 (w), 861 (m), 826 (w) cm^{-1}. UV-Vis (DMSO, λ_{max} (nm (ε $M^{-1}cm^{-1}$))): 403.01 (15124), 532 (1465), 659.70 (6333.8).

Synthesis of $[Ni_4(L_{Br})_4Cl_4(H_2O)_4]$ (**3**)

$NiCl_2$ (26 mg, 0.2 mmol) and 5-bromo-2-pyridinemethanol (L_{Br}, 38 mg, 0.2 mmol) were added to the mixture of MeOH/MeCN (10 mL, *v*/*v* = 1:1). The mixture was sealed in a Pyrex glass tube and smoothly heated to 105 °C within 2 h, and maintained for 72 h before cooling to room temperature in 24 h to give dark-green block single crystals. The dark-green crystals were filtered, then washed with Et_2O and dried in vacuo. Yield: 31.6 mg (52.8% based on Ni). Anal. Calcd. (%) for $C_{24}H_{28}Br_4Cl_4N_4Ni_4O_8$: C 24.06, H 2.34, N 4.68; found: C 24.14, H 2.78, N 4.99. IR (KBr

disc): 3239 (m), 2903 (w), 2837 (m), 1591 (m), 1473 (s), 1382 (m), 1344 (w), 1282 (m), 1095 (s), 1065 (s), 1032 (m), 833 (w) cm^{-1}. UV-Vis (DMSO, λ_{max} (nm (ε $M^{-1}cm^{-1}$))): 407.03 (40167.5), 532 (1865), 663.42 (16763.5).

Synthesis of $[Ni_4(L_{Cl})_4Br_4(EtOH)_4]$ (**4**)

A mixture of $NiBr_2{\cdot}6H_2O$ (65 mg, 0.2 mmol), 4-chloro-2-pyridinemethanol (L_{Cl}, 29 mg, 0.1 mmol) and EtOH (10 mL) was sealed in a Pyrex glass tube and smoothly heated to 120 °C within 2 h, and maintained for 48 h before cooling to room temperature in 24 h to give light-green plate single crystals. The light-green plate crystals are filtered, washed with EtOH, and dried in vacuo. Yield: 28 mg (42.8% based on Ni). Anal. Calcd. (%) for $C_{32}H_{44}Br_4Cl_4N_4Ni_4O_8$: C 29.34, H 3.36, N 4.28; found: C 29.21, H 3.58, N 4.36. IR (KBr disc): 3259 (s), 3074 (w), 2966 (w), 2898 (w), 2850 (w), 1593 (s), 1553 (m), 1470 (m), 1403 (m), 1069 (s), 1049 (w), 879 (w) cm^{-1}. UV-Vis (DMSO, λ_{max} (nm (ε $M^{-1}cm^{-1}$))): 403.94 (17333.5), 532 (1665), 658.72(7144.9).

Synthesis of $[Ni_4(L_{Br})_4Br_4(MeOH)_4]$ (**5**)

A mixture of $NiBr_2{\cdot}6H_2O$ (65 mg, 0.2 mmol), 5-bromo-2-pyridinemethanol (L_{Br}, 38 mg, 0.2 mmol) and MeOH/MeCN (10 mL, *v*/*v* = 1:1) was sealed in a Pyrex glass tube and smoothly heated to 120 °C within 2 h, maintained for 48 h before cooling to room temperature in 24 h to give light-green plate single crystals. The light-green crystals were filtered, then washed with Et_2O and dried in vacuo. Yield: 27 mg (41.3% based on Ni). Anal. Calcd. (%) for $C_{28}H_{32}Br_8N_4Ni_4O_8$: C 23.67, H 2.92, N 20.70; found: C 23.97, H 3.12, N 20.21. IR (KBr disc): 3463(s), 3370 (s), 3047(w), 2847 (w), 1590 (m), 1474 (s), 1383 (m), 1285(m), 1070 (s), 1030 (s), 834 (w) cm^{-1}. UV-Vis (DMSO, λ_{max} (nm (ε $M^{-1}cm^{-1}$))): 403.01 (27938), 532 (1065), 657.4 (11888.6).

2. Third−order nonlinear optical (NLO) measurements

Compounds **1**−**5** were stable in air and laser light under experimental conditions. Solutions of these compounds in DMSO (1.0×10^{-4} M) were placed in a 2 mm quartz cuvette for the third-order NLO measurements. The nonlinear absorption and

refraction were investigated with a linear polarized laser light (λ = 532 nm; pulse width = 15 ps, repetition rate = 10 Hz) generated from a frequency-doubled, mode-locked, Q-switched Nd: YAG laser. The transmittance of light (T) is a function of the sample's Z position (with respect to the focal point at Z = 0), the nonlinear absorption [$\alpha = \beta(I_i)$] and the linear absorption (α_0) are described by Eq. 1. In addition, the trough-peak separation (ΔZ_{V-P}) and the difference between normalized transmittance values at the trough and peak positions (ΔT_{V-P}) fit the following two equations (Eqs 2, 3), which originate for a third-order NLO process (Eq. 2). The effective third-order NLO refractive index n_2 (Eq. 3) can be derived from ΔT_{V-P}. The calculation formulas of α_2 (nonlinear absorptive index), n_2 (third-order NLO refractive index), $\chi^{(3)}$ (third-order susceptibility), and γ (hyperpolarizability) are listed as Eqs. 4−7, where τ is the time, α_0, L, I, and λ are the linear coefficient, the sample thickness, the peak irradiation intensity at the focus, and the wavelength of the laser, respectively. N is the density a unit number of molecules per cubic centimeters and n_0 is the linear refractive index of DMSO (n_0 = 1.48).

$$T(Z) = \frac{\alpha_0}{\sqrt{\pi}\beta I_i(Z)(1 - e^{-\alpha_0 L})} \int_{-\infty}^{\infty} \ln\left[1 + \beta I_i(Z) \frac{1 - e^{-\alpha_0 L}}{\alpha_0} e^{-\tau^2}\right] d\tau \quad (1)$$

$$\Delta Z_{V-P} = 1.72\pi\omega_0^2 / \lambda \quad (2)$$

$$n_2^{eff} = \lambda\alpha_0\Delta T_{V-P} / \left[0.812\pi I\left(1 - e^{\alpha L}\right)\right] \quad (3)$$

$$\chi_I^{(3)} = 9 \times 10^8 \varepsilon_0 n_0^2 c^2 \beta / (4\omega\pi) \quad (4)$$

$$\chi_R^{(3)} = c n_0^2 n_2 / (80\pi) \quad (5)$$

$$\chi^{(3)} = [(\chi_I^{(3)})^2 + (\chi_R^{(3)})^2]^{1/2} \quad (6)$$

$$\gamma = \chi^{(3)} / [N((n_0^2 + 2)/3)^4] \quad (7)$$

3. DFT Calculations

The density functional theory (DFT) calculations were performed using Gaussian 09 program,[1] with cluster models directly inherited from the experimental X-ray single-crystal structure data without further optimization. The HOMO/LUMO orbitals and their energies in DMSO solution were calculated at the B3LYP/LanL2DZ level using the polarized continuum model (PCM).

4. X-ray structure determination

All measurements were made on a Bruker D8-Quest (**1**, **2**, **4** and **5**) and an Agilent Xcalibur (**3**) CCD X-ray diffractometer using an enhanced X-ray source Mo Kα (λ = 0.71073 Å). Cell parameters were refined using the programs Bruker SAINT (for **1**, **2**, **4** and **5**) and *CrysAlisPro* (Agilent Technologies, Ver. 1.171.35.21, 2012) (for **3**). Absorption corrections (multi-scan) were applied to all complexes.[2] All crystal structures were solved by direct methods and refined on F_2 by full-matrix least-squares methods with the *SHELXTL-2013* program.[3] For **1**, The hydrogen atoms on O atoms of the coordinated MeOH were located from the difference Fourier map with their O–H distances restrained to be equal and thermal parameters constrained to U_{iso}(H) = 1.2U_{eq}(O). In **2**, the coordinates of the hydrogen atoms on the OH of coordinated EtOH were suggested by Calc-OH program in WinGX suite,[4] with the OH group subsequently refined as a rigid group with thermal parameters constrained to U_{iso}(H) = 1.2U_{eq}(O). In **3**, the locations of the hydrogen atoms on the coordinated water were suggested by Calc-OH program in WinGX suite,[4] and the water molecules were subsequently refined as a rigid group with their O–H distances were further restrained to O–H = 0.83 Å and thermal parameters constrained to U_{iso}(H) = 1.2U_{eq}(O). In **4**, the hydrogen atoms on the OH of coordinated EtOH were located from the difference Fourier map with their O–H distances restrained to O–H = 0.83 Å and thermal parameters constrained to U_{iso}(H) = 1.2U_{eq}(O). In **5**, the locations of the two hydrogen atoms on the coordinated water were suggested by Calc-OH program in WinGX suite,[4] their O–H distances were further restrained to O–H = 0.83 Å and thermal parameters constrained to U_{iso}(H) = 1.2U_{eq}(O). Some amount of spatially

delocalized electron density in the lattice of **1** – **3**, and **5** were found but acceptable refinement results could not be obtained for this electron density. The solvent contribution was then modeled using SQUEEZE in the Platon program suite.[5] Crystallographic data have been deposited with the Cambridge Crystallographic Data Center (CCDC) (1826295−1826299). A summary of crystal data and structure refinement parameters of **1**−**5** are given in Table S1 and the selected bond lengths and angles are listed in Table S2.

5. Tables S1−S5

Table S1 Crystal data and structure refinement parameters for **1**–**5**

Compounds	**1**	**2**
Formula	$C_{28}H_{44}Cl_4N_8Ni_4O_8$	$C_{32}H_{44}Cl_8N_4Ni_4O_8$
Formula Weight	997.35	1113.15
Crystal System	Monoclinic	Monoclinic
Space Group	*C*2/*c*	$P2_1/n$
a/Å	29.842(3)	16.035(2)
b/Å	14.8679(11)	16.5596(19)
c/Å	24.7389(18)	18.461(2)
α/°	90	90
β/°	116.734(2)	111.804(4)
γ/°	90	90
V/Å^3	9803.0(14)	4551.2(10)
Z	8	4
ρ_{calc} /(g cm^{-3})	1.352	1.651
F(000)	4096	2304
μ (Mo–Ka)/mm^{-1}	1.776	2.148
Total Reflections	100674	58520
Unique Reflections	12178	58520
No. Observations	9621	36940
No. Parameters	485	481
R_{int}	0.0513	0.1310
R^a	0.0284	0.0981
wR^b	0.0650	0.2187
GOF^c	1.005	1.038

Table S1 continued

3	**4**	**5**
$C_{24}H_{28}Br_4Cl_4N_4Ni_4O_8$	$C_{32}H_{44}Br_4Cl_4N_4Ni_4O_8$	$C_{28}H_{36}Br_8N_4Ni_4O_8$
1196.78	1308.99	1430.73
Orthorhombic	Tetragonal	Monoclinic
$C222_1$	$I4_1/acd$	$P2_1/c$
16.4251(8)	16.899(3)	12.204(3)
17.2816(13)	16.899(3)	17.407(4)
17.0414(17)	32.661(9)	24.119(5)
90	90	90
90	90	94.966(6)
90	90	90
4837.2(6)	9327 (4)	5104.8(19)
4	8	4
1.643	1.864	1.862
2336	5184	2752
5.096	3.249	7.754
10114	201966	12490
5264	2907	8795
3482	2489	6536
217	130	445
0.0567	0.1505	0.1396
0.0620	0.0808	0.1003
0.1474	0.2849	0.2211
0.999	1.154	1.038

Table S2 Selected bond lengths (Å) and angles (°) for **1**–**5**

Compound 1			
Ni(1)-N(1)	2.0294(16)	Ni(2)-N(3)	2.0234(16)
Ni(3)-N(5)	2.0380(16)	Ni(4)-N(7)	2.0289(16)
Ni(1)-O(2)	2.0510(13)	Ni(2)-O(4)	2.0489(13)
Ni(1)-O(1)	2.0510(12)	Ni(2)-O(2)	2.0632(13)
Ni(1)-O(4)	2.0950(13)	Ni(2)-O(3)	2.0925(13)
Ni(1)-O(5)	2.1350(15)	Ni(2)-O(6)	2.1235(14)
Ni(3)-O(3)	2.0480(13)	Ni(4)-O(3)	2.0429(13)
Ni(3)-O(1)	2.0545(12)	Ni(4)-O(4)	2.0562(12)
Ni(3)-O(2)	2.0921(13)	Ni(4)-O(1)	2.1000(13)
Ni(3)-O(7)	2.1136(14)	Ni(4)-O(8)	2.1260(14)
Ni(1)-Cl(1)	2.3635(5)	Ni(2)-Cl(2)	2.3917(6)
Ni(3)-Cl(3)	2.4013(5)	Ni(4)-Cl(4)	2.3875(5)
N(1)-Ni(1)-O(2)	162.51(6)	N(5)-Ni(3)-O(2)	101.67(6)
N(1)-Ni(1)-O(1)	81.49(6)	O(3)-Ni(3)-O(2)	78.68(5)
O(2)-Ni(1)-O(1)	82.43(5)	O(1)-Ni(3)-O(2)	81.34(5)
N(1)-Ni(1)-O(4)	101.80(6)	N(5)-Ni(3)-O(7)	90.01(6)
O(2)-Ni(1)-O(4)	81.81(5)	O(3)-Ni(3)-O(7)	96.74(5)
O(1)-Ni(1)-O(4)	79.13(5)	O(1)-Ni(3)-O(7)	85.52(5)
N(1)-Ni(1)-O(5)	85.13(6)	O(2)-Ni(3)-O(7)	166.53(5)
O(2)-Ni(1)-O(5)	88.57(6)	N(5)-Ni(3)-Cl(3)	96.60(5)
O(1)-Ni(1)-O(5)	91.85(5)	O(3)-Ni(3)-Cl(3)	174.01(4)
O(4)-Ni(1)-O(5)	167.56(5)	O(1)-Ni(3)-Cl(3)	100.08(4)
N(1)-Ni(1)-Cl(1)	97.06(5)	O(2)-Ni(3)-Cl(3)	96.34(4)
O(2)-Ni(1)-Cl(1)	99.66(4)	O(7)-Ni(3)-Cl(3)	88.85(4)
O(1)-Ni(1)-Cl(1)	173.60(4)	N(7)-Ni(4)-O(3)	162.87(6)
O(4)-Ni(1)-Cl(1)	95.12(4)	N(7)-Ni(4)-O(4)	81.26(6)
O(5)-Ni(1)-Cl(1)	94.25(4)	O(3)-Ni(4)-O(4)	81.91(5)
N(3)-Ni(2)-O(4)	163.48(6)	N(7)-Ni(4)-O(1)	98.24(6)
N(3)-Ni(2)-O(2)	80.98(6)	O(3)-Ni(4)-O(1)	81.57(5)
O(4)-Ni(2)-O(2)	82.63(5)	O(4)-Ni(4)-O(1)	78.90(5)
N(3)-Ni(2)-O(3)	97.78(6)	N(7)-Ni(4)-O(8)	91.25(6)
O(4)-Ni(2)-O(3)	80.89(5)	O(3)-Ni(4)-O(8)	87.09(5)
O(2)-Ni(2)-O(3)	78.33(5)	O(4)-Ni(4)-O(8)	95.07(5)
N(3)-Ni(2)-O(6)	90.57(6)	O(1)-Ni(4)-O(8)	167.78(5)

O(4)-Ni(2)-O(6)	88.75(5)	N(7)-Ni(4)-Cl(4)	98.81(5)
O(2)-Ni(2)-O(6)	94.94(5)	O(3)-Ni(4)-Cl(4)	98.14(4)
O(3)-Ni(2)-O(6)	168.25(5)	O(8)-Ni(4)-Cl(4)	87.27(4)
N(3)-Ni(2)-Cl(2)	98.91(5)	O(6)-Ni(2)-Cl(2)	89.23(4)
O(4)-Ni(2)-Cl(2)	97.59(4)	N(5)-Ni(3)-O(3)	81.30(6)
O(2)-Ni(2)-Cl(2)	175.83(4)	N(5)-Ni(3)-O(1)	162.63(6)
O(3)-Ni(2)-Cl(2)	97.58(4)	O(3)-Ni(3)-O(1)	82.56(5)
Compound 2			
Ni(1)-O(1)	2.037(7)	Ni(3)-O(1)	2.033(8)
Ni(1)-N(1)	2.067(10)	Ni(3)-O(3)	2.046(8)
Ni(1)-O(4)	2.069(8)	Ni(3)-N(3)	2.057(10)
Ni(1)-O(5)	2.073(9)	Ni(3)-O(7)	2.081(9)
Ni(1)-O(2)	2.098(8)	Ni(3)-O(4)	2.099(8)
Ni(1)-Cl(5)	2.354(3)	Ni(3)-Cl(7)	2.359(4)
Ni(2)-O(2)	2.031(8)	Ni(4)-O(4)	2.022(8)
Ni(2)-O(3)	2.067(8)	Ni(4)-O(2)	2.034(8)
Ni(2)-O(6)	2.068(9)	Ni(4)-N(4)	2.053(10)
Ni(2)-N(2)	2.073(10)	Ni(4)-O(3)	2.098(8)
Ni(2)-O(1)	2.094(8)	Ni(4)-O(8)	2.110(9)
Ni(2)-Cl(6)	2.346(3)	Ni(4)-Cl(8)	2.328(4)
O(1)-Ni(1)-N(1)	79.8(3)	O(1)-Ni(1)-O(4)	82.0(3)
N(1)-Ni(1)-O(4)	160.8(4)	O(1)-Ni(1)-O(5)	95.9(3)
N(1)-Ni(1)-O(5)	90.0(4)	O(4)-Ni(1)-O(5)	85.8(3)
O(1)-Ni(1)-O(2)	79.5(3)	N(1)-Ni(1)-O(2)	102.1(4)
O(4)-Ni(1)-O(2)	80.5(3)	O(5)-Ni(1)-O(2)	165.9(3)
O(1)-Ni(1)-Cl(5)	171.9(3)	N(1)-Ni(1)-Cl(5)	96.8(3)
O(4)-Ni(1)-Cl(5)	102.0(2)	O(5)-Ni(1)-Cl(5)	91.4(3)
O(2)-Ni(1)-Cl(5)	94.1(2)	O(2)-Ni(2)-O(3)	82.0(3)
O(2)-Ni(2)-O(6)	93.5(4)	O(3)-Ni(2)-O(6)	87.5(3)
O(2)-Ni(2)-N(2)	79.3(3)	O(3)-Ni(2)-N(2)	160.6(4)
O(6)-Ni(2)-N(2)	88.6(4)	O(2)-Ni(2)-O(1)	79.7(3)
O(3)-Ni(2)-O(1)	80.4(3)	O(6)-Ni(2)-O(1)	166.8(3)
N(2)-Ni(2)-O(1)	101.1(3)	O(3)-Ni(2)-Cl(6)	101.5(2)
O(2)-Ni(2)-Cl(6)	173.1(3)	O(6)-Ni(2)-Cl(6)	92.7(3)
N(2)-Ni(2)-Cl(6)	97.7(3)	O(3)-Ni(3)-N(3)	79.5(4)
O(1)-Ni(2)-Cl(6)	94.8(2)	O(1)-Ni(3)-O(7)	88.8(3)
O(1)-Ni(3)-O(3)	82.4(3)	O(3)-Ni(3)-O(7)	91.9(4)
O(1)-Ni(3)-N(3)	161.6(4)	N(3)-Ni(3)-O(7)	88.7(4)

O(1)-Ni(3)-O(4)	81.4(3)	O(3)-Ni(3)-O(4)	79.5(3)
N(3)-Ni(3)-O(4)	98.3(3)	O(7)-Ni(3)-O(4)	167.7(4)
O(1)-Ni(3)-Cl(7)	101.0(2)	O(4)-Ni(3)-Cl(7)	95.4(2)
O(3)-Ni(3)-Cl(7)	173.5(2)	O(4)-Ni(4)-O(2)	83.2(3)
N(3)-Ni(3)-Cl(7)	97.3(3)	O(4)-Ni(4)-N(4)	80.4(4)
O(7)-Ni(3)-Cl(7)	93.7(3)	O(2)-Ni(4)-N(4)	162.3(4)
O(4)-Ni(4)-O(3)	80.1(3)	O(2)-Ni(4)-O(8)	88.3(3)
O(2)-Ni(4)-O(3)	81.2(3)	N(4)-Ni(4)-O(8)	86.0(4)
N(4)-Ni(4)-O(3)	102.3(4)	O(3)-Ni(4)-O(8)	168.0(3)
O(4)-Ni(4)-O(8)	93.0(4)	O(4)-Ni(4)-Cl(8)	172.7(3)
O(2)-Ni(4)-Cl(8)	99.9(2)	O(3)-Ni(4)-Cl(8)	93.7(2)
N(4)-Ni(4)-Cl(8)	97.2(3)	O(8)-Ni(4)-Cl(8)	93.8(3)

Compound 3

Ni(1)-O(1)	2.043(7)	Ni(2)-O(1)	2.063(6)
Ni(1)-O(2)#1	2.055(6)	Ni(2)-O(2)#1	2.096(7)
Ni(1)-N(1)	2.089(8)	Ni(2)-O(2W)	2.100(9)
Ni(1)-O(1W)	2.103(9)	Ni(2)-Cl(2)	2.361(4)
Ni(1)-O(1)#1	2.104(7)	O(1)-Ni(1)#1	2.104(7)
Ni(1)-Cl(1)	2.350(3)	O(2)-Ni(1)#1	2.055(6)
Ni(2)-O(2)	2.038(7)	O(2)-Ni(2)#1	2.096(7)
Ni(2)-N(2)	2.054(8)	O(1)-Ni(1)-O(2)#1	82.9(3)
O(1)-Ni(1)-N(1)	79.5(3)	O(2)#1-Ni(1)-Cl(1)	99.0(2)
O(2)#1-Ni(1)-N(1)	161.8(3)	N(1)-Ni(1)-Cl(1)	99.0(3)
O(1)-Ni(1)-O(1W)	93.0(4)	O(1W)-Ni(1)-Cl(1)	92.1(3)
O(2)#1-Ni(1)-O(1W)	88.9(3)	O(1)#1-Ni(1)-Cl(1)	95.3(2)
N(1)-Ni(1)-O(1W)	87.6(4)	O(2)-Ni(2)-N(2)	79.9(3)
O(1)-Ni(1)-O(1)#1	79.9(3)	O(2)-Ni(2)-O(1)	82.4(3)
O(2)#1-Ni(1)-O(1)#1	81.0(3)	N(2)-Ni(2)-O(1)	161.5(3)
N(1)-Ni(1)-O(1)#1	100.0(3)	O(2)-Ni(2)-O(2)#1	80.5(3)
O(1W)-Ni(1)-O(1)#1	168.3(3)	N(2)-Ni(2)-O(2)#1	101.3(3)
O(1)-Ni(1)-Cl(1)	174.6(2)	O(1)-Ni(2)-O(2)#1	81.4(3)
O(1)-Ni(2)-O(2W)	87.0(3)	O(2W)-Ni(2)-Cl(2)	93.0(3)
O(2)#1-Ni(2)-O(2W)	167.2(3)	O(1)-Ni(2)-Cl(2)	101.2(2)
O(2)-Ni(2)-Cl(2)	173.4(2)	O(2)#1-Ni(2)-Cl(2)	94.5(2)
N(2)-Ni(2)-Cl(2)	96.9(3)	N(2)-Ni(2)-O(2W)	88.1(4)

Symmetry transformations used to generate equivalent atoms: #1 *x*, –*y*, –*z* + 1.

Compound 4

Br(1)-Ni(1)	2.5190(14)	Ni(1)-O(2)	2.091(8)
Ni(1)-O(1)	2.048(6)	Ni(1)-O(1)#2	2.111(6)
Ni(1)-O(1)#1	2.060(5)	O(1)-Ni(1)#3	2.060(5)
Ni(1)-N(1)	2.067(7)	O(1)-Ni(1)#2	2.111(6)
O(1)-Ni(1)-O(1)#1	81.7(2)	O(1)#1-Ni(1)-O(2)	89.0(3)
O(1)-Ni(1)-N(1)	80.0(2)	N(1)-Ni(1)-O(2)	87.2(3)
O(1)#1-Ni(1)-N(1)	161.0(3)	O(1)-Ni(1)-O(1)#2	79.9(3)
O(1)-Ni(1)-O(2)	92.5(3)	O(1)#1-Ni(1)-O(1)#2	80.2(2)
N(1)-Ni(1)-O(1)#2	101.1(3)	O(2)-Ni(1)-O(1)#2	167.6(3)
O(1)-Ni(1)-Br(1)	173.52(17)	N(1)-Ni(1)-Br(1)	96.5(2)
O(1)#1-Ni(1)-Br(1)	102.24(17)	O(2)-Ni(1)-Br(1)	92.7(2)
O(1)#2-Ni(1)-Br(1)	95.57(16)		

Symmetry transformations used to generate equivalent atoms: #1 *y* + 1/4, –*x* + 3/4, –*z* + 1/4; #2 –*x* + 1, –*y* + 1/2, *z* + 0; #3 –*y* + 3/4, *x* – 1/4, –*z* + 1/4.

Compound 5

Ni(1)-O(1)	2.043(10)	Ni(3)-O(2)	2.043(8)
Ni(1)-N(1)	2.058(11)	Ni(3)-N(3)	2.052(12)
Ni(1)-O(3)	2.067(9)	Ni(3)-O(4)	2.097(9)
Ni(1)-O(5)	2.107(12)	Ni(3)-O(7)	2.109(12)
Ni(1)-O(2)	2.109(10)	Ni(3)-Br(3)	2.519(2)
Ni(1)-Br(1)	2.519(2)	Ni(4)-O(4)	2.055(9)
Ni(2)-O(4)	2.044(8)	Ni(4)-O(1)	2.072(9)
Ni(2)-O(2)	2.044(9)	Ni(4)-N(4)	2.098(11)
Ni(2)-N(2)	2.055(10)	Ni(4)-O(8)	2.104(11)
Ni(2)-O(1)	2.088(9)	Ni(4)-O(3)	2.122(9)
Ni(2)-O(6)	2.097(11)	Ni(4)-Br(4)	2.503(2)
Ni(2)-Br(2)	2.524(2)	O(1)-Ni(1)-N(1)	79.1(4)
Ni(3)-O(3)	2.035(9)	O(1)-Ni(1)-O(3)	82.5(4)
N(1)-Ni(1)-O(3)	161.3(4)	O(2)-Ni(1)-Br(1)	95.9(3)
O(1)-Ni(1)-O(5)	93.4(5)	O(4)-Ni(2)-O(2)	82.1(3)
N(1)-Ni(1)-O(5)	89.6(5)	O(4)-Ni(2)-N(2)	160.5(4)
O(3)-Ni(1)-O(5)	88.3(4)	O(2)-Ni(2)-N(2)	79.6(4)
O(1)-Ni(1)-O(2)	79.9(4)	O(4)-Ni(2)-O(1)	81.5(3)
N(1)-Ni(1)-O(2)	98.5(4)	O(2)-Ni(2)-O(1)	80.3(4)
O(3)-Ni(1)-O(2)	81.2(3)	N(2)-Ni(2)-O(1)	101.8(4)
O(5)-Ni(1)-O(2)	168.2(4)	O(4)-Ni(2)-O(6)	87.2(4)

O(1)-Ni(1)-Br(1)	173.8(3)	O(2)-Ni(2)-O(6)	93.4(5)
N(1)-Ni(1)-Br(1)	97.2(3)	N(2)-Ni(2)-O(6)	87.2(5)
O(3)-Ni(1)-Br(1)	101.4(3)	O(1)-Ni(2)-O(6)	167.7(4)
O(5)-Ni(1)-Br(1)	91.6(4)	O(4)-Ni(2)-Br(2)	101.5(3)
O(2)-Ni(2)-Br(2)	175.1(3)	O(3)-Ni(3)-O(7)	93.4(5)
N(2)-Ni(2)-Br(2)	97.2(3)	O(2)-Ni(3)-O(7)	89.2(4)
O(1)-Ni(2)-Br(2)	96.8(3)	N(3)-Ni(3)-O(7)	89.4(5)
O(6)-Ni(2)-Br(2)	90.2(4)	O(4)-Ni(3)-O(7)	168.8(4)
O(3)-Ni(3)-O(2)	83.6(4)	O(3)-Ni(3)-Br(3)	176.9(3)
O(3)-Ni(3)-N(3)	80.3(4)	O(2)-Ni(3)-Br(3)	98.8(3)
O(2)-Ni(3)-N(3)	163.8(5)	N(3)-Ni(3)-Br(3)	97.4(4)
O(3)-Ni(3)-O(4)	80.5(4)	O(4)-Ni(3)-Br(3)	97.9(3)
O(2)-Ni(3)-O(4)	80.8(3)	O(7)-Ni(3)-Br(3)	88.6(4)
N(3)-Ni(3)-O(4)	98.7(4)	O(4)-Ni(4)-O(1)	81.7(3)
O(4)-Ni(4)-N(4)	80.0(4)	O(4)-Ni(4)-Br(4)	174.1(3)
O(1)-Ni(4)-N(4)	160.7(4)	O(1)-Ni(4)-Br(4)	100.5(3)
O(4)-Ni(4)-O(8)	93.1(4)	N(4)-Ni(4)-Br(4)	98.3(3)
O(1)-Ni(4)-O(8)	90.0(5)	O(8)-Ni(4)-Br(4)	92.4(4)
N(4)-Ni(4)-O(8)	85.1(5)	O(3)-Ni(4)-Br(4)	95.5(3)
O(4)-Ni(4)-O(3)	79.5(3)	N(4)-Ni(4)-O(3)	101.8(4)
O(1)-Ni(4)-O(3)	80.5(4)	O(8)-Ni(4)-O(3)	168.6(4)

Table S3 Hydrogen bonding tables for **1**–**5**

D-H···A	D-H (Å)	H···A (Å)	D···A (Å)	∠D-H···A (°)
Compound 1				
O5-H1O5···Cl3	0.795(14)	2.249(15)	3.0301(15)	167(2)
O6-H1O6···Cl1	0.797(13)	2.193(14)	2.9791(16)	169(2)
O7-H1O7···Cl4	0.796(13)	2.239(14)	3.0222(15)	168(2)
O8-H1O8···Cl2	0.802(14)	2.246(15)	3.0268(15)	165(2)
N2-H2A···Cl2	0.88	2.70	3.520(2)	156.0#1
N4-H4B···Cl1	0.88	2.89	3.544(2)	132.7#2
N6-H6A···Cl4	0.88	2.76	3.550(2)	149.3#3
N8-H8A···Cl3	0.88	2.62	3.477(2)	164.6#4
N8-H8B···Cl3	0.88	2.48	3.3361(19)	163.6#5
Symmetry codes for generating equivalent atoms: #1 –*x* + 1/2, *y* + 1/2, –*z* + 1/2; #2 –*x* + 1/2, –*y* + 3/2, –*z* + 1; #3 –*x*, *y*, –*z* + 1/2; #4 –*x* + 1/2, *y* – 1/2, –*z* + 1/2; #5 *x*, –*y* + 2, *z* – 1/2.				
Compound 2				
O5-H1O5···Cl7	0.83	2.33	3.065(10)	148.4
O6-H1O6···Cl8	0.83	2.39	3.001(9)	130.8
O7-H1O7···Cl6	0.83	2.27	3.059(10)	158.3
O8-H1O8···Cl5	0.83	2.25	3.040(11)	158.6
Compound 3				
O1W-H2W1···Cl2	0.83	2.25	3.056(11)	164.4
O2W-H2W2···Cl1	0.83	2.29	3.025(10)	147.1#1
O2W-H2W2···O1	0.83	2.40	2.865(11)	116.3
Symmetry codes for generating equivalent atoms: #1 *x*, –*y*, –*z* + 1.				
Compound 4				
O2-H1O2···Br1	0.82(2)	2.40(5)	3.189(7)	160(11)#1
Symmetry codes for generating equivalent atoms: #1 –*y* + 3/4, *x* – 1/4, –*z* + 1/4.				
Compound 5				
O5-H1O5···Br4	0.83	2.31	3.142(13)	179.7
O6-H1O6···Br3	0.83	2.34	3.168(12)	179.7
O7-H1O7···Br1	0.83	2.30	3.134(13)	179.9
O8-H1O8···Br2	0.83	2.33	3.158(13)	179.9

Table S4 The third-order NLO parameters of **1**–**5**

	T_0 (%)	α_2 (10^{-13} m W^{-1})	n_2 (10^{-20} m^2 W^{-1})	$\chi_I^{(3)}$ (10^{-15} esu)	$\chi_R^{(3)}$ (10^{-14} esu)	$\chi^{(3)}$ (10^{-14} esu)	γ (10^{-34} esu)
1	88	1.10	−2.0	3.87	−1.66	1.71	0.75
2	92	0.30	–	1.06	–	0.11	0.05
3	93	0.50	1.0	1.76	0.83	0.85	0.37
4	92	0.70	−5.0	2.46	−4.16	4.17	1.82
5	87	0.30	−5.0	1.06	4.16	4.16	1.82

Table S5 List of relevant HOMO and LUMO orbital energies and band gaps for **1**–**5** calculated by DFT.

	HOMO −2 (ev)	HOMO −1 (ev)	HOMO (ev)	LUMO (ev)	LUMO +1 (ev)	LUMO +2 (ev)	E-gap (HOMO -LUMO) (ev)	Relevant MLCT gap(nm)
1	−4.61723	−4.29777	−4.20443	−2.29202	−2.08385	−2.06072	1.912417192	648.31
2	−4.78295	−4.65424	−4.42076	−2.61175	−2.50481	−2.41773	1.809013872	685.37
3	−5.10704	−5.04200	−4.79764	−2.82373	−2.79352	−2.77611	1.973914956	628.11
4	−4.98839	−4.69315	−4.59301	−2.78237	−2.56277	−2.56086	1.810646556	684.75
5	−5.12119	−4.82295	−4.74676	−2.99026	−2.80386	−2.73556	1.75649587	705.86

6. Figures S1–S7

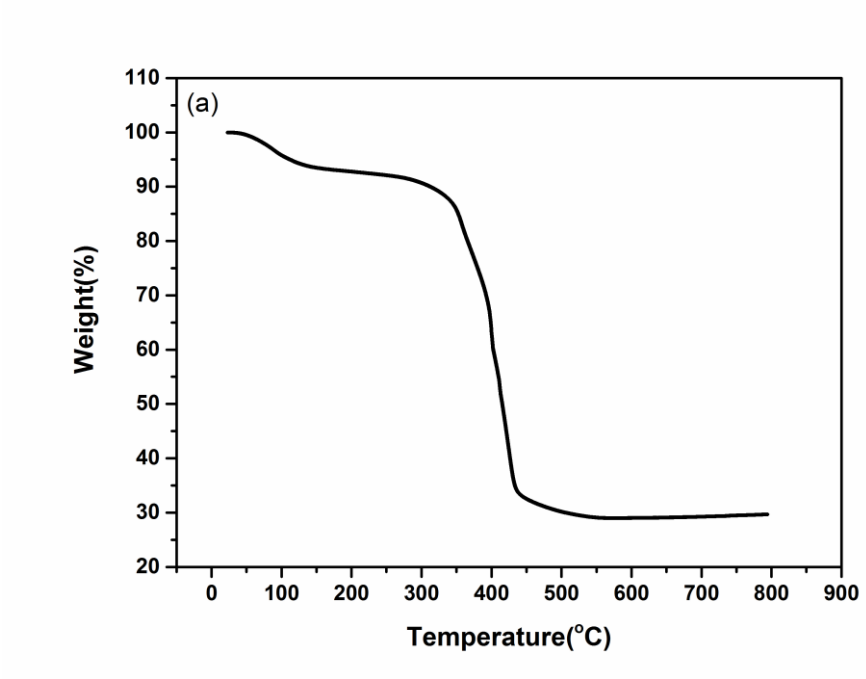

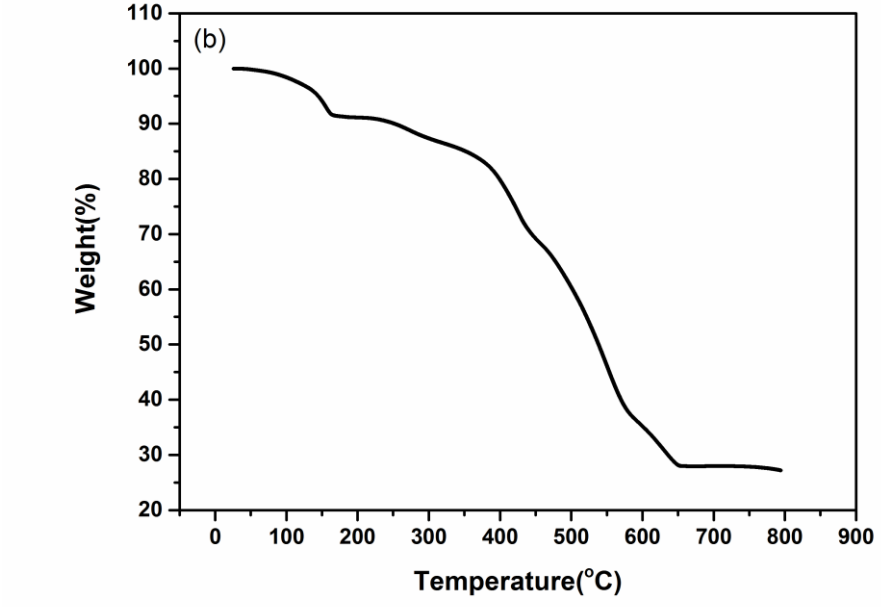

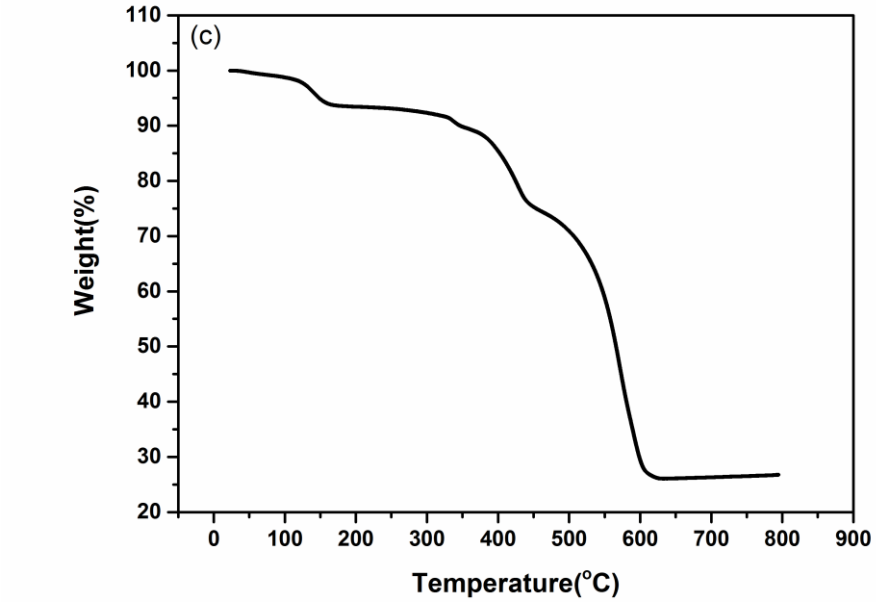
(c)
Weight(%)
Temperature(°C)
110
100
90
80
70
60
50
40
30
20
0
100
200
300
400
500
600
700
800
900

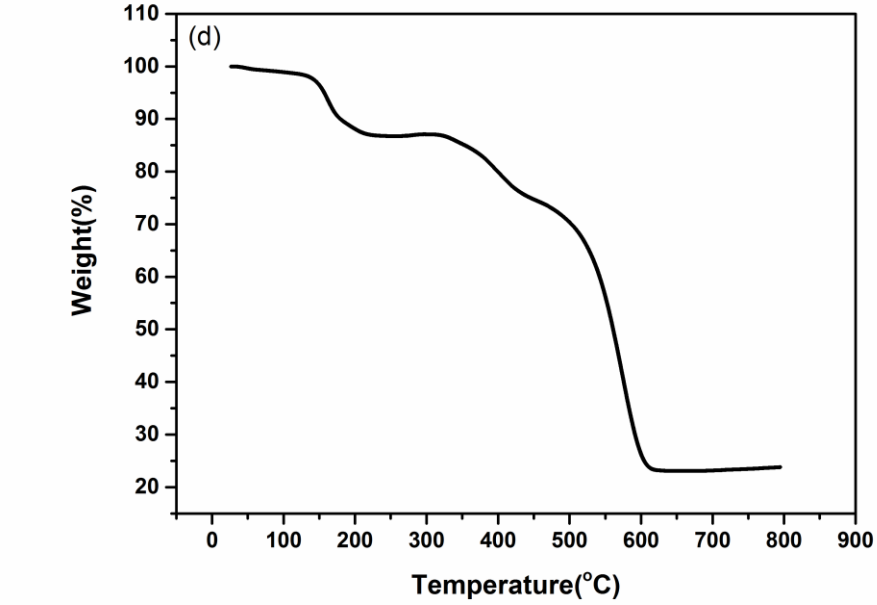
(d)
Weight(%)
Temperature(°C)
110
100
90
80
70
60
50
40
30
20
0
100
200
300
400
500
600
700
800
900

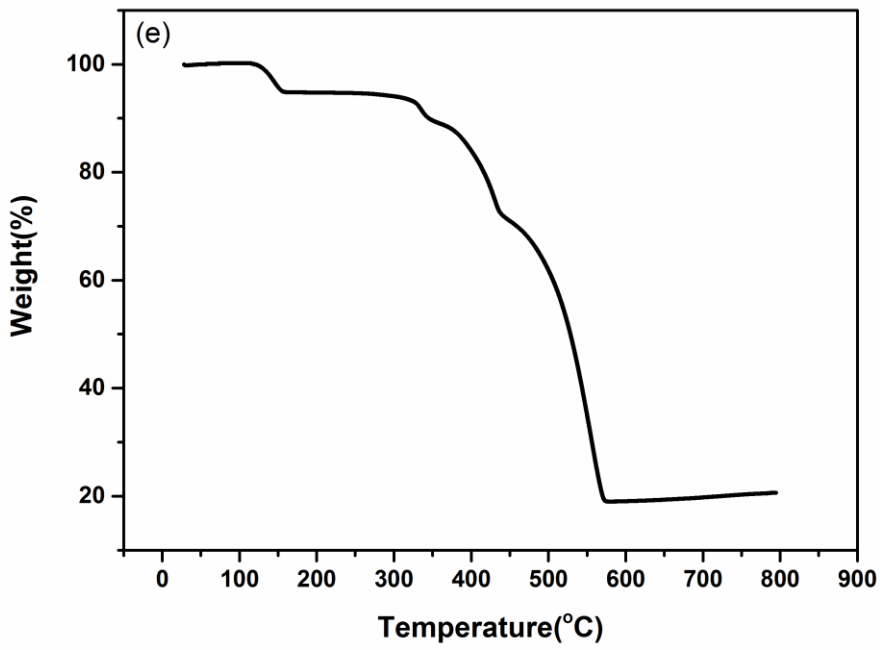

Fig. S1 The TGA spectra of compounds **1** (a), **2** (b), **3** (c), **4** (d), **5** (e) in an O_2 atmosphere.

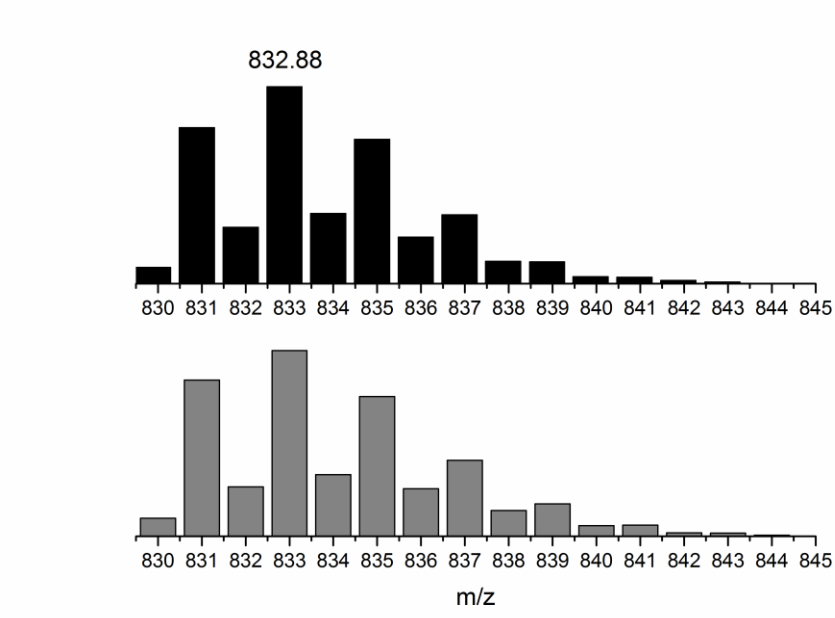

(a)

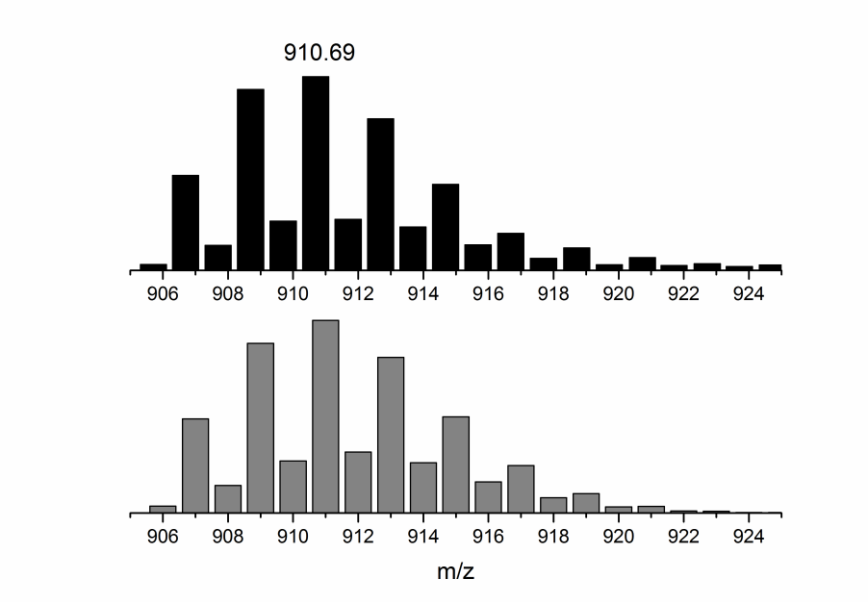
910.69
906 908 910 912 914 916 918 920 922 924
906 908 910 912 914 916 918 920 922 924
m/z

(b)

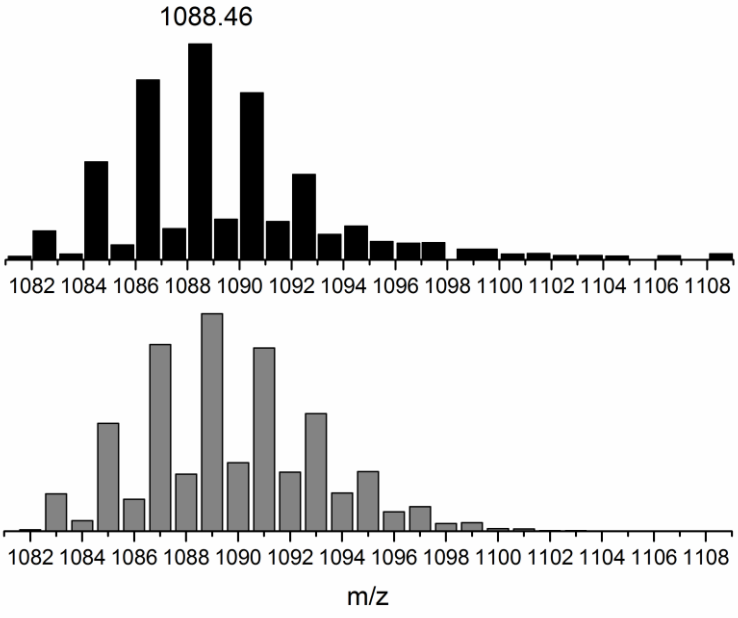
1088.46
1082 1084 1086 1088 1090 1092 1094 1096 1098 1100 1102 1104 1106 1108
1082 1084 1086 1088 1090 1092 1094 1096 1098 1100 1102 1104 1106 1108
m/z

(c)

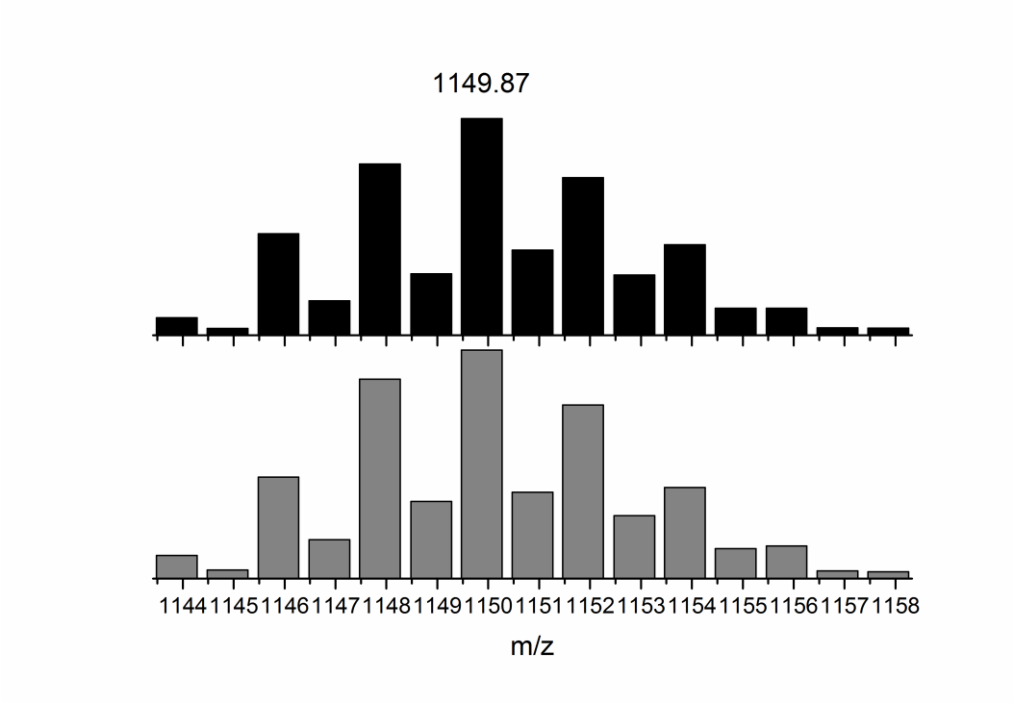

(d)

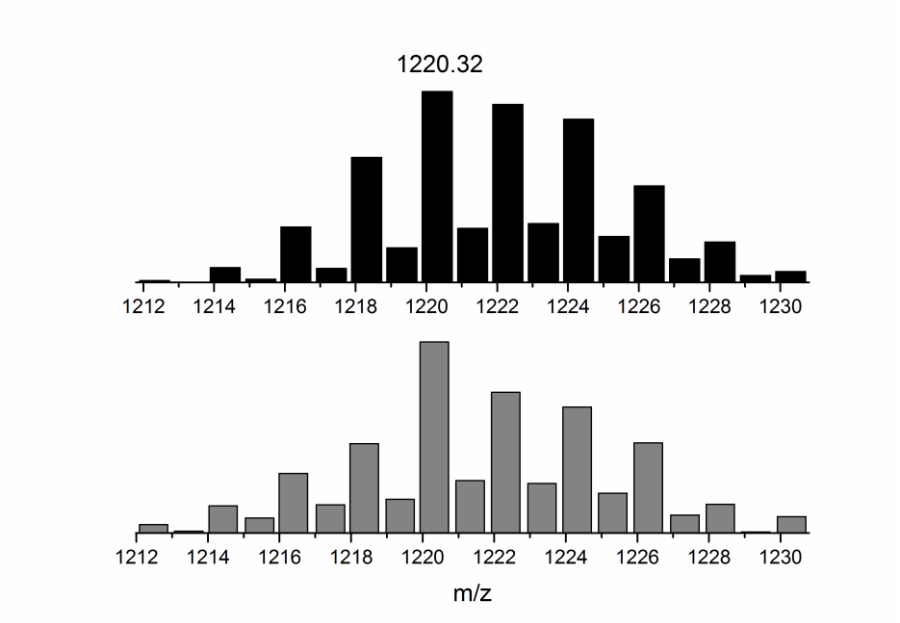

(e)

Fig. S2 The positive-ion ESI-MS patterns (top) and the calculated isotope patterns (below) of the $[Ni_4\mathbf{L}_4Cl_3]^+$ cation in **1** (a), $[Ni_4\mathbf{L}_4Cl_3]^+$ cation in **2** (b), $\{[Ni_4\mathbf{L}_4Cl_2]+OH^-+H_2O\}^+$ cation in **3** (c), $\{[Ni_4Br_3\mathbf{L}_4]+MeOH\}^+$ cation in **4** (d), and $[Ni_4\mathbf{L}_4Br_3]^+$ cation in **5** (e).

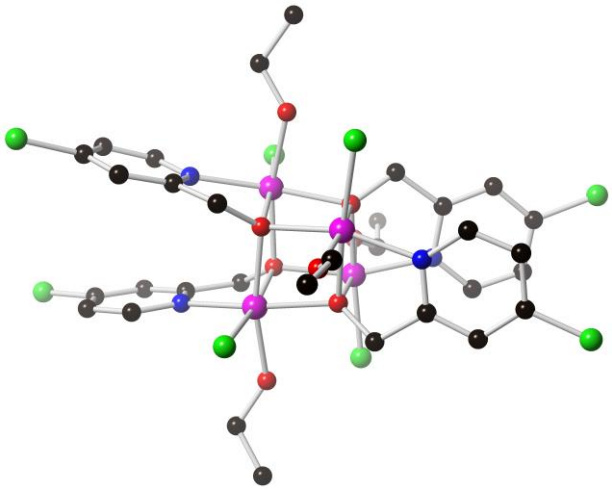

(a)

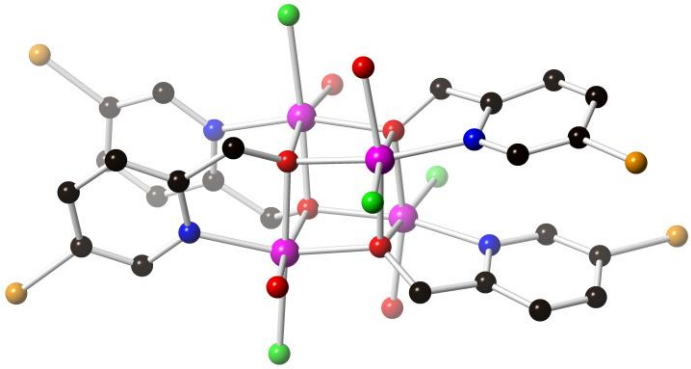

(b)

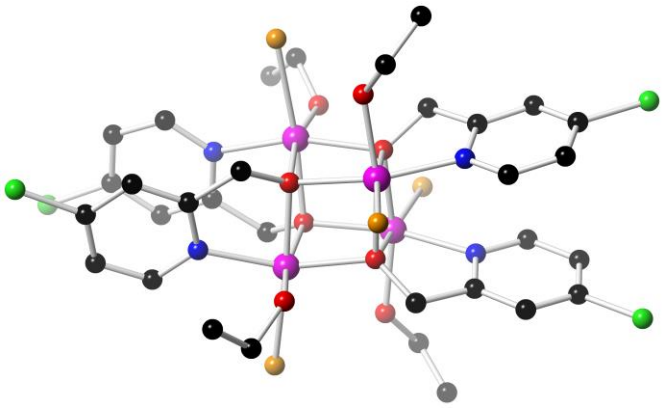

(c)

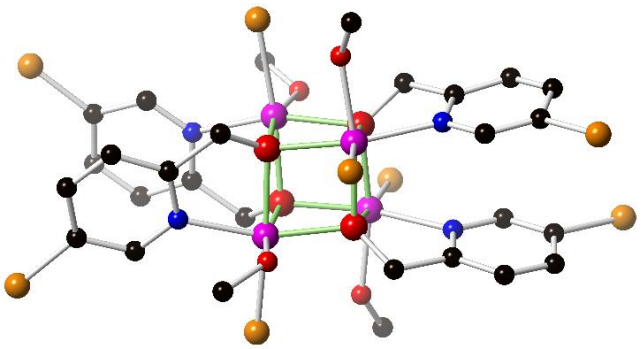

(d)

Fig. S3 The structures of **2** (a), **3** (b), **4** (c) and **5** (d) with the disordered components, lattice solvates, and hydrogen atoms omitted. Color codes: Ni (magenta), O (red), N (blue), C (black), Cl (green), Br (orange).

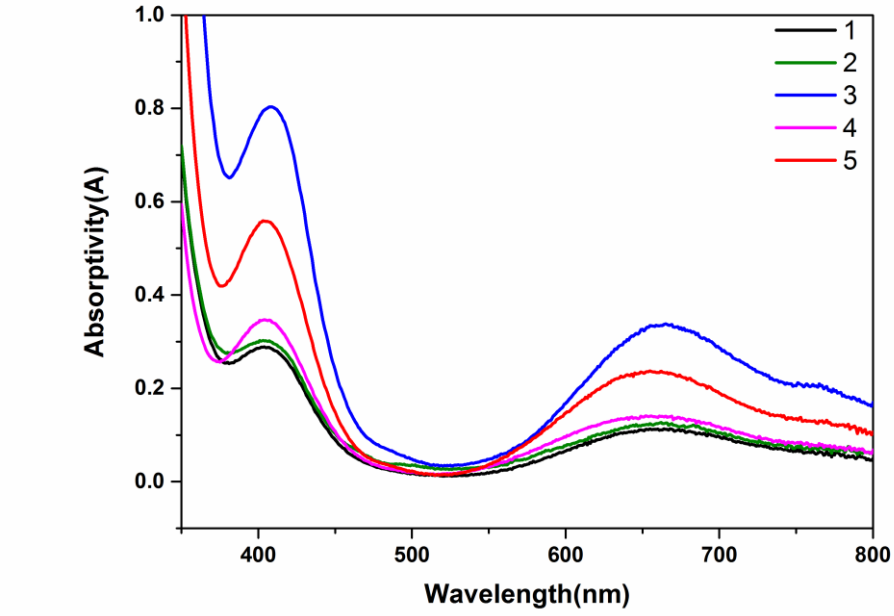

(a)

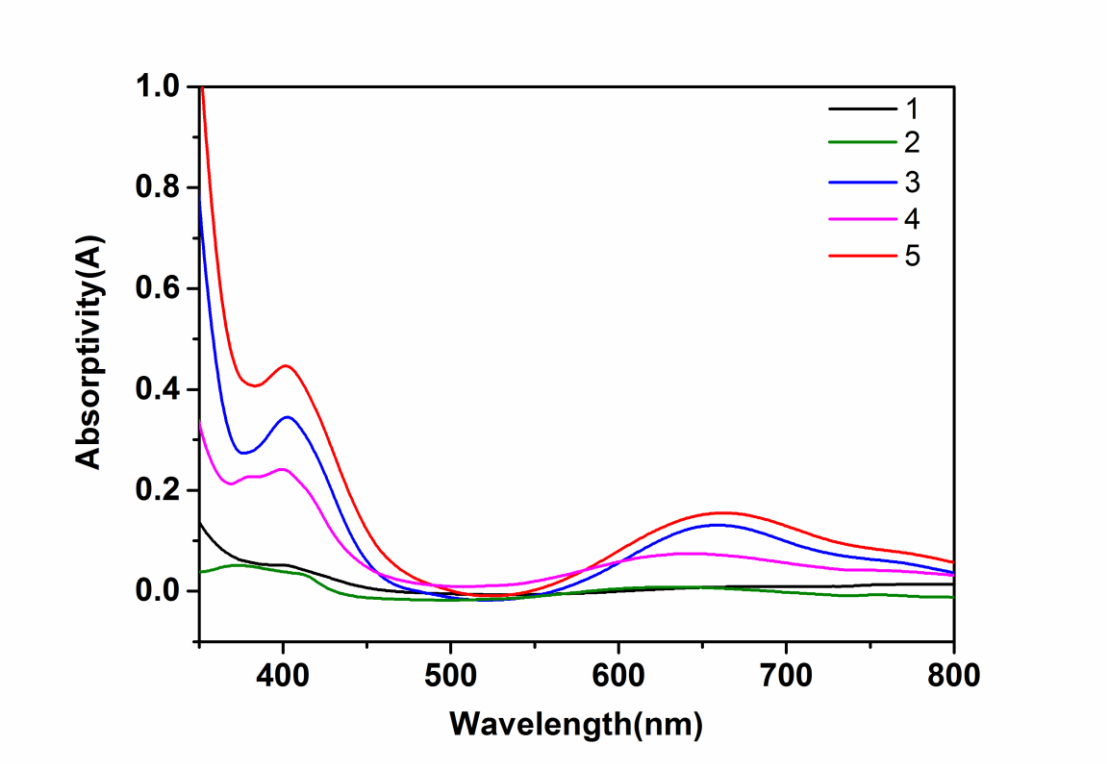

(b)

Fig. S4 The UV-Vis spectra of **1**–**5** in DMSO (1×10^{-4} M) solution (a) and those after NLO experiments (b).

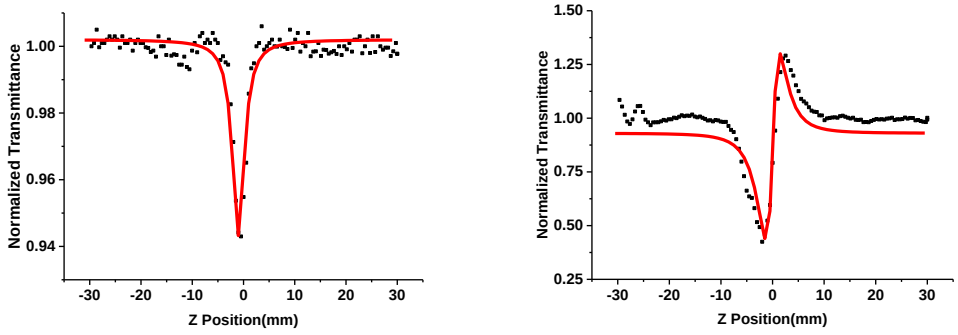

(1a) (1b)

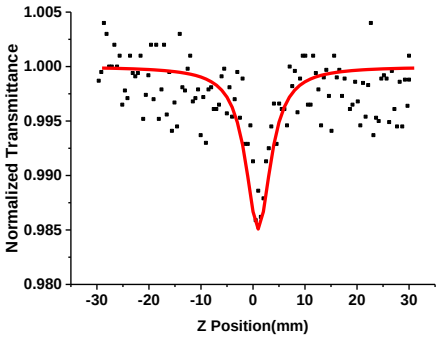

(2a)

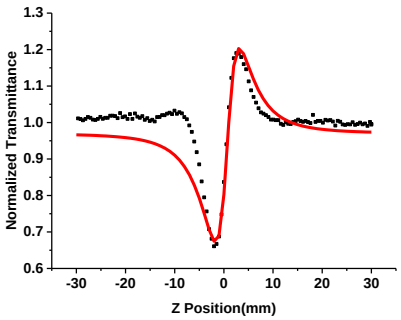

(2b)

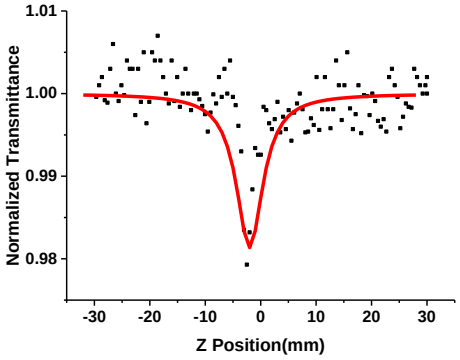

(3a)

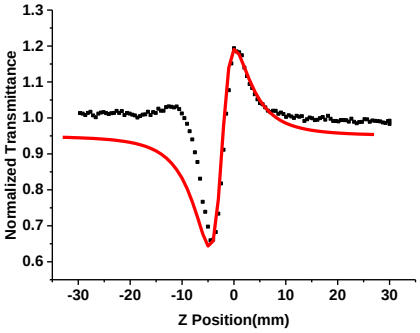

(3b)

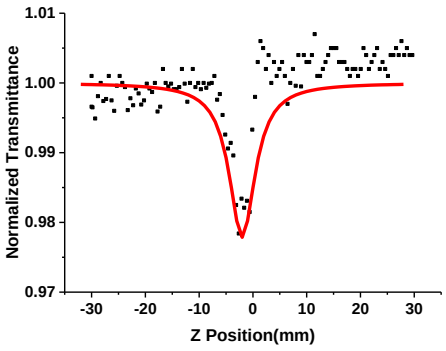

(4a)

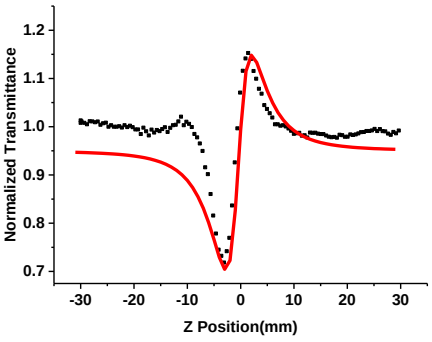

(4b)

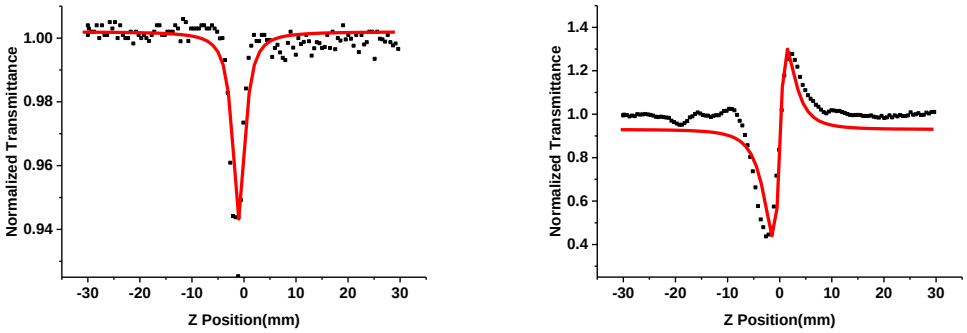

(5a) (5b)

Fig. S5 The Z-scan data for **1**–**5** (1×10^{-4} M) in DMSO solution investigated at 532 nm. (a) Normalized Z-scan data obtained using an open-aperture configuration showing the nonlinear absorption; (b) collected by dividing the normalized Z-scan data of the refractive part. The black solid squares are experimental data, and the red solid curves theoretical fits.

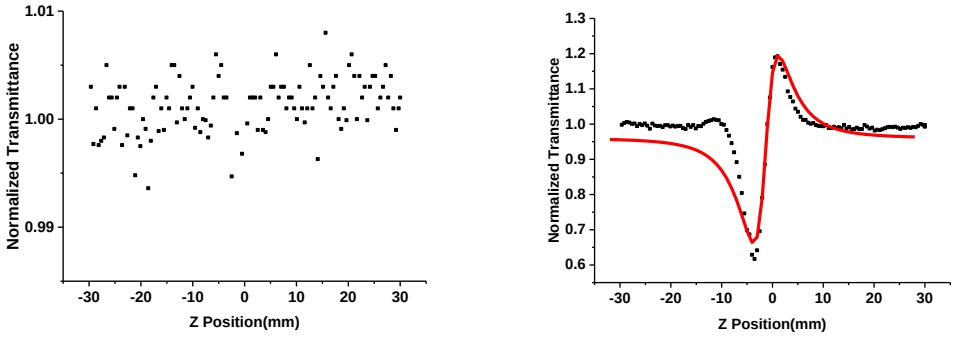

(a) (b)

Fig. S6 The Z-scan data for the blank DMSO solution investigated at 532 nm. (a) Z-scan data obtained using an open-aperture configuration; (b) collected by dividing the normalized Z-scan data of the refractive part. The black solid squares are experimental data, and the red solid curves theoretical fit.

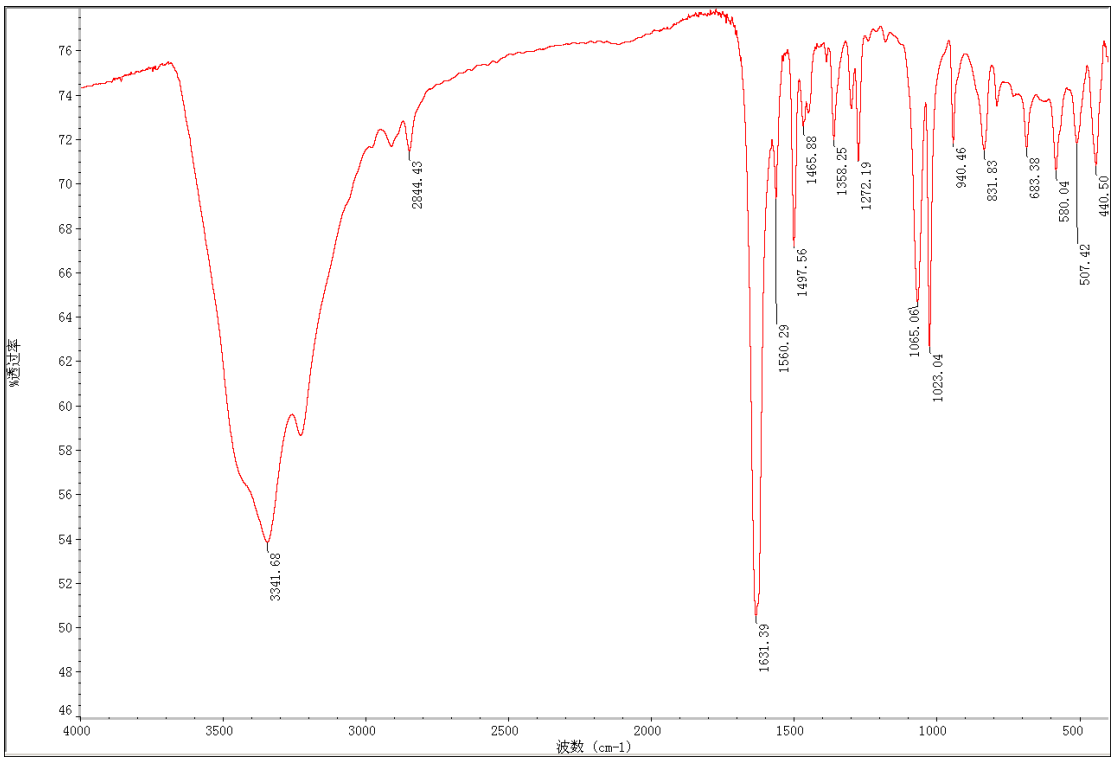
%透过率
波数（cm-1）
3341.68
2844.43
1631.39
1560.29
1497.56
1465.88
1358.25
1272.19
1065.06
1023.04
940.46
831.83
683.38
580.04
507.42
440.50

(a1)


%透过率
波数（cm-1）
3335.38
1642.09
1632.41
1560.20
1498.62
1467.14
1444.90
1383.87
1358.68
1271.58
1065.42
1022.60

(a2)


%透过率
波数（cm-1）
3363.04
2899.39
2841.48
1594.94
1555.92
1472.60
1403.52
1343.41
1285.45
1205.52
1078.59
1020.85
861.19
826.11
734.82
720.50
666.45
636.79
546.21
508.92
437.15

(b1)

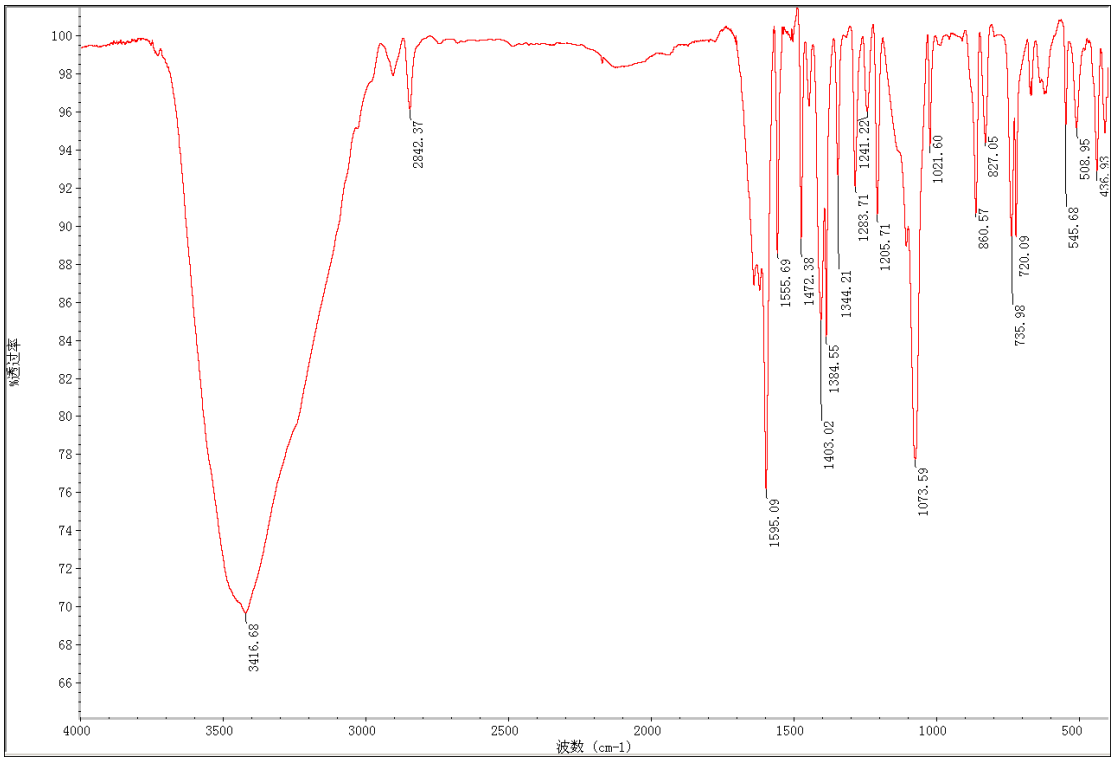
%透过率
波数（cm-1）
3416.68
2842.37
1595.09
1555.69
1472.38
1403.02
1384.55
1344.21
1283.71
1241.22
1205.71
1073.59
1021.60
860.57
827.05
735.98
720.09
545.68
508.95
436.93

(b2)

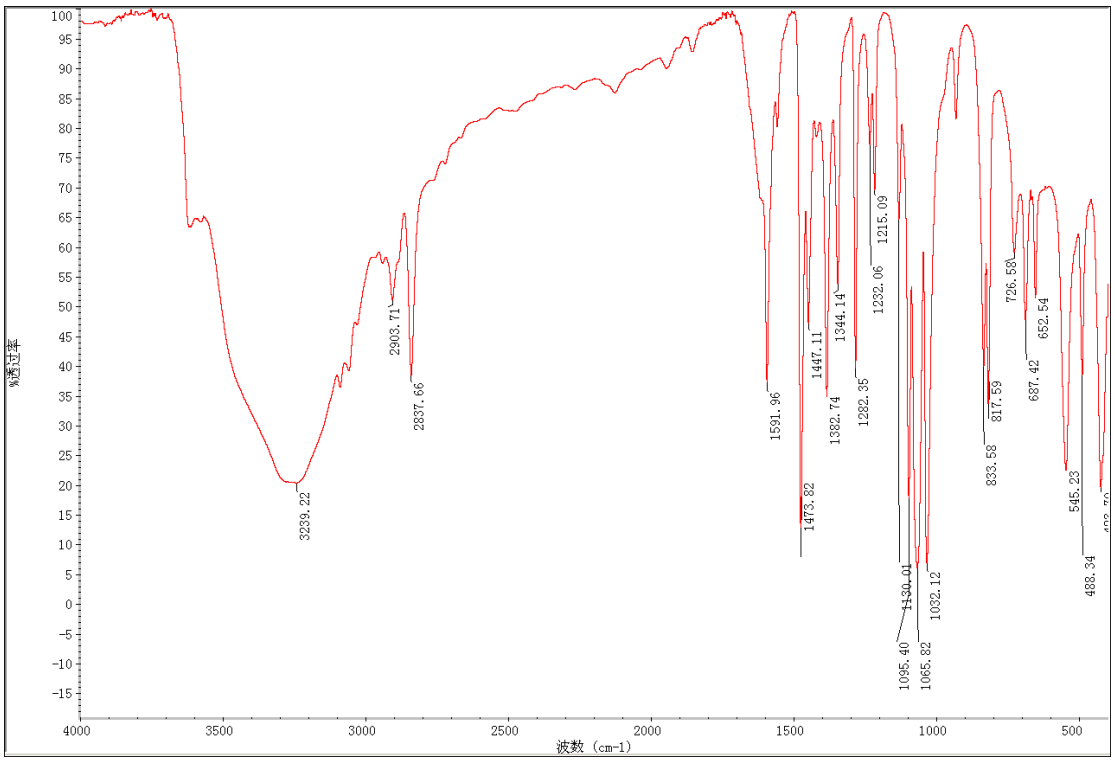
%透过率
波数（cm-1）
3239.22
2903.71
2837.66
1591.96
1473.82
1447.11
1382.74
1344.14
1282.35
1232.06
1215.09
1130.01
1095.40
1065.82
1032.12
833.58
817.59
726.58
687.42
652.54
545.23
488.34

(c1)

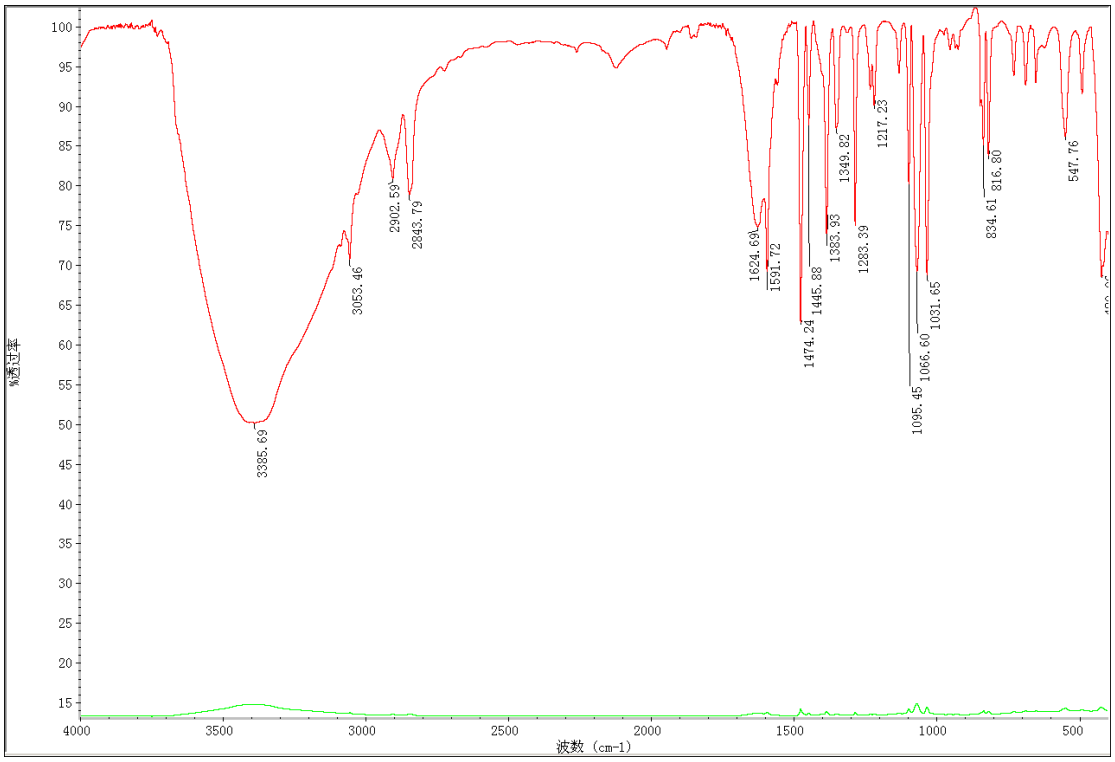
%透过率
波数（cm-1）
3385.69
3053.46
2902.59
2843.79
1624.69
1591.72
1474.24
1445.88
1383.93
1349.82
1283.39
1217.23
1095.45
1066.60
1031.65
834.61
816.80
547.76

(c2)


%透过率
波数 (cm-1)
3259.58
3074.38
2966.37
2898.16
2850.36
1593.64
1553.03
1470.48
1444.83
1403.89
1346.50
1278.08
1241.18
1207.44
1069.24
1049.02
1020.27
879.32
858.85
844.22
740.71
720.19
669.32
548.45
505.71
436.95

(d1)


%透过率
波数 (cm-1)
3482.84
3246.09
2967.76
2897.63
2849.69
1594.03
1553.19
1470.86
1445.25
1402.99
1384.81
1346.30
1278.79
1241.21
1207.74
1068.41
1020.40
859.52
843.98
740.99
720.29
669.18
615.83
547.99
505.69
437.90

(d2)


%透过率
波数 (cm-1)
3463.59
3370.63
3047.99
2915.98
2847.89
1590.81
1474.22
1383.82
1285.33
1070.23
1030.96
834.88
816.47
685.86
650.44
553.12
461.98

(e1)

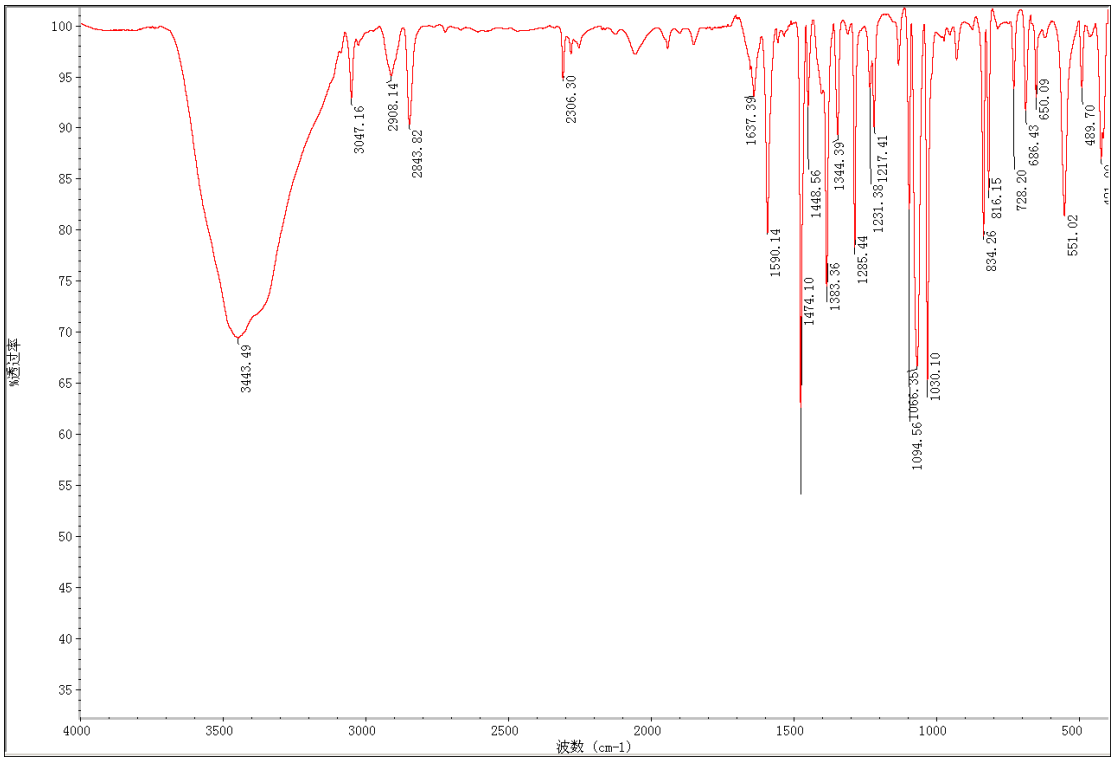
%透过率
波数 (cm-1)
3443.49
3047.16
2908.14
2843.82
2306.30
1637.39
1590.14
1474.10
1448.56
1383.36
1344.39
1285.44
1231.38
1217.41
1094.56
1066.35
1030.10
834.26
816.15
728.20
686.43
650.09
551.02
489.70

(e2)

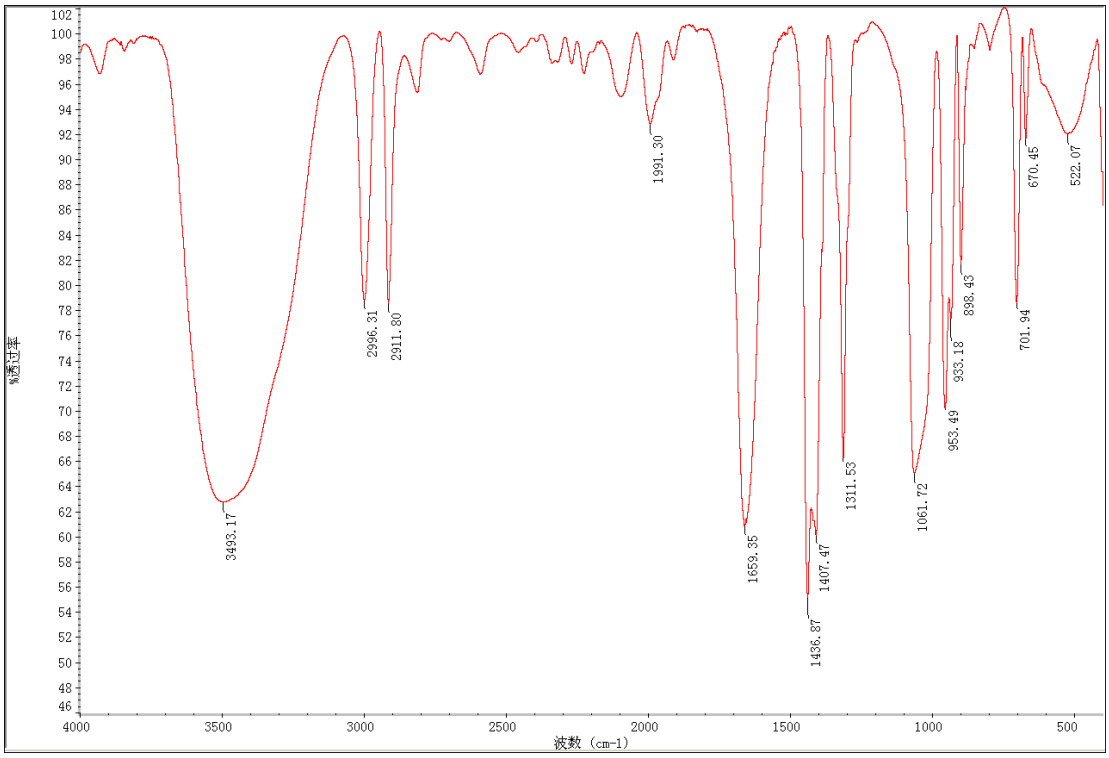

(f)

Fig. S7 The IR spectra of compounds **1**–**5** (a1) – (e1), those upon treatment with MeCN/DMSO (a2) – (e2), as well as the blank DMSO (f).

Compound **1**		
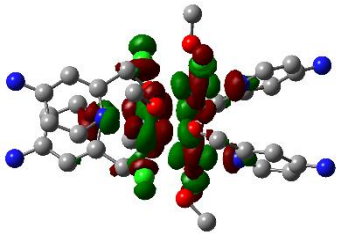	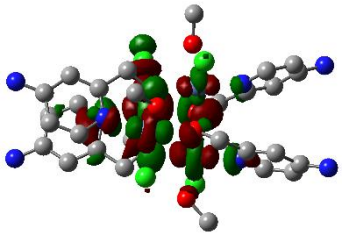	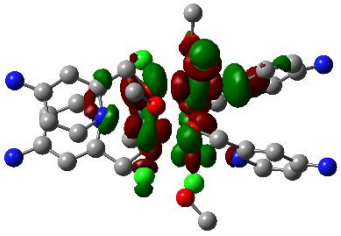
LUMO	LUMO +1	LUMO +2
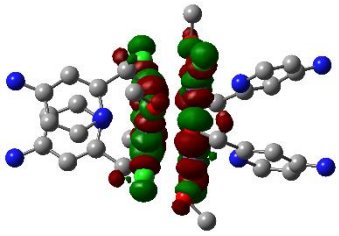	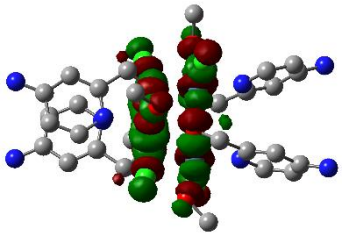	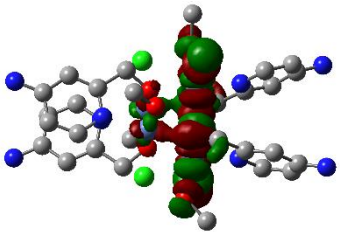
HOMO	HOMO −1	HOMO −2
Compound **2**		

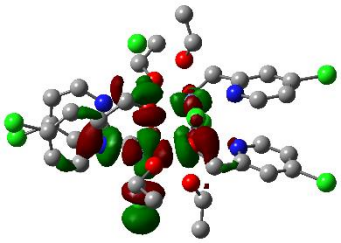	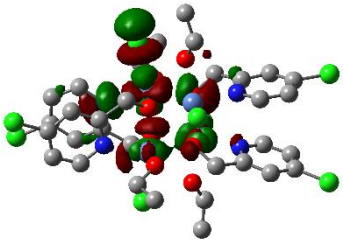	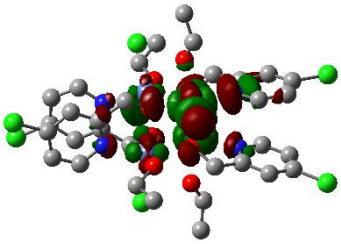
LUMO	LUMO +1	LUMO +2
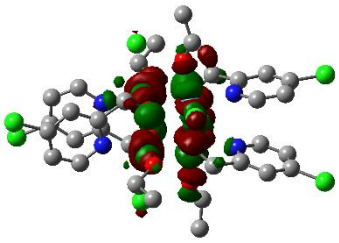	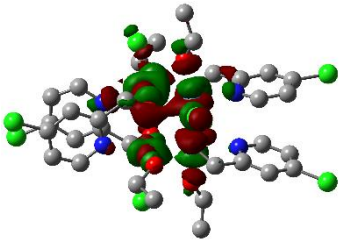	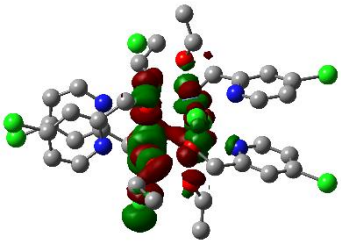
HOMO	HOMO −1	HOMO −2
Compound **3**		
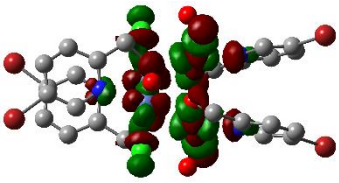	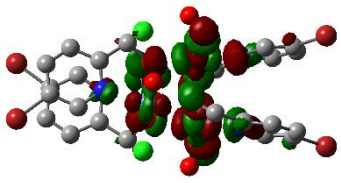	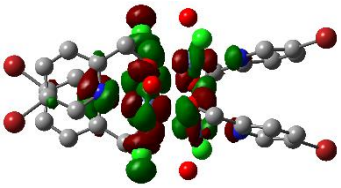
LUMO	LUMO +1	LUMO +2
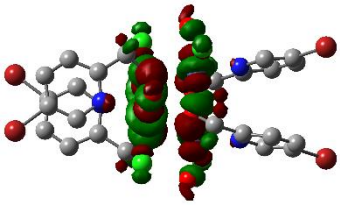	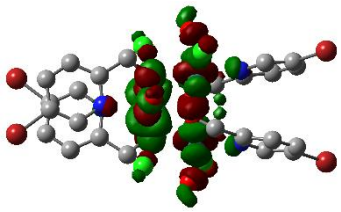	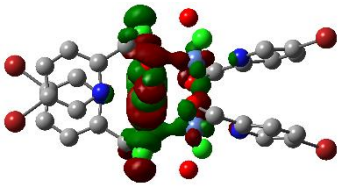
HOMO	HOMO −1	HOMO −2
Compound **4**		
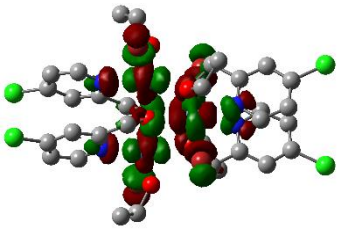	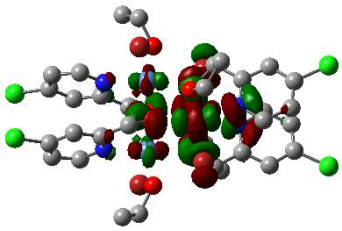	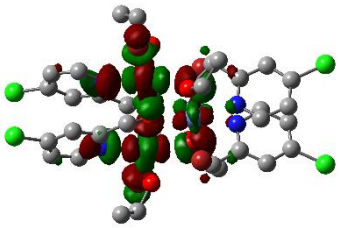
LUMO	LUMO +1	LUMO +2
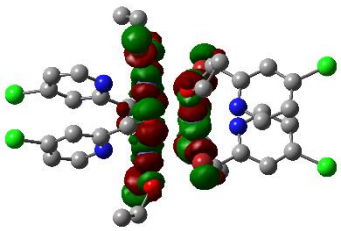	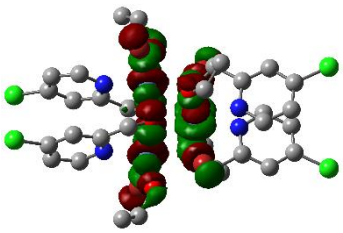	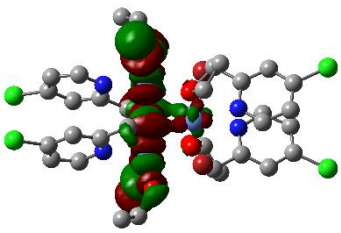
HOMO	HOMO −1	HOMO −2
Compound **5**		

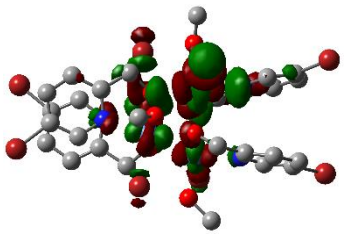	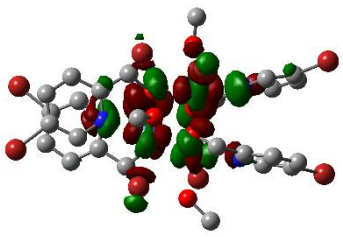	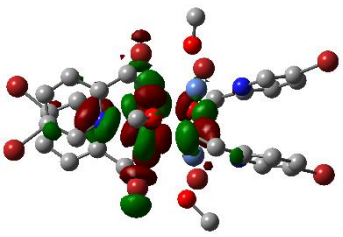
LUMO	LUMO +1	LUMO +2
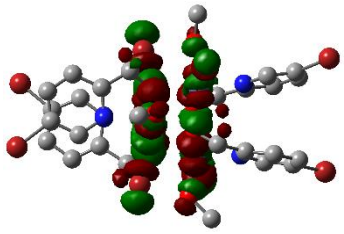	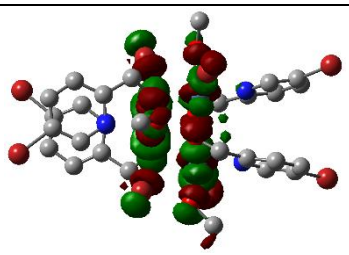	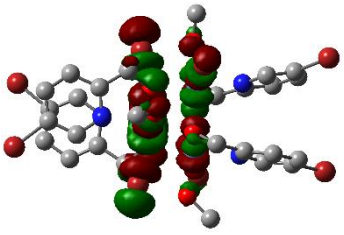
HOMO	HOMO −1	HOMO −2

Fig. S8 The LUMO and HOMO figures for **1**−**5**.

7. References

1. Gaussian 09, Revision A.02, M. J. Frisch, G. W. Trucks, H. B. Schlegel, G. E. Scuseria, M. A. Robb, J. R. Cheeseman, G. Scalmani, V. Barone, G. A. Petersson, H. Nakatsuji, X. Li, M. Caricato, A. Marenich, J. Bloino, B. G. Janesko, R. Gomperts, B. Mennucci, H. P. Hratchian, J. V. Ortiz, A. F. Izmaylov, J. L. Sonnenberg, D. Williams-Young, F. Ding, F. Lipparini, F. Egidi, J. Goings, B. Peng, A. Petrone, T. Henderson, D. Ranasinghe, V. G. Zakrzewski, J. Gao, N. Rega, G. Zheng, W. Liang, M. Hada, M. Ehara, K. Toyota, R. Fukuda, J. Hasegawa, M. Ishida, T. Nakajima, Y. Honda, O. Kitao, H. Nakai, T. Vreven, K. Throssell, J. A. Montgomery, Jr., J. E. Peralta, F. Ogliaro, M. Bearpark, J. J. Heyd, E. Brothers, K. N. Kudin, V. N. Staroverov, T. Keith, R. Kobayashi, J. Normand, K. Raghavachari, A. Rendell, J. C. Burant, S. S. Iyengar, J. Tomasi, M. Cossi, J. M. Millam, M. Klene, C. Adamo, R. Cammi, J. W. Ochterski, R. L. Martin, K. Morokuma, O. Farkas, J. B. Foresman, and D. J. Fox, Gaussian, Inc., Wallingford CT, 2016.
2. G. M. Sheldrick, *SADABS: Program for empirical absorption correction of area detector data; University of Göttingen, Germany*, 1996.
3. G. Sheldrick, *Acta Crystallogr., Sect. C*, 2015, **71**, 3−8.
4. L. J. Farrugia, *J. Appl. Crystallogr.*, 2012, **45**, 849−854.
5. A. L. Spek, *Acta Crystallogr., Sect. C*, 2015, **71**, 9−18.